Environmental Modelling and Software 191 (2025) 106497

Contents lists available at ScienceDirect

Environmental Modelling and Software

journal homepage: www.elsevier.com/locate/envsoft

Integrated hydrological modeling and analysis tool for automatic derivation of design floods in Sicilian watersheds

Antonio Francipane [a,*], Giuseppe Cipolla [b], Dario Treppiedi [a], Leonardo Valerio Noto [a]

[a] *Engineering Department at the University of Palermo, Palermo, Italy*
[b] *AECOM, Milano, Italy*

ARTICLE INFO

Keywords:
Design flood modeling
Hydrological modeling
GIS
Spatial distribution of flow velocities across a watershed
Sicily

ABSTRACT

This work presents a tool that enhances the hydrological flood modeling process at the event scale by integrating geospatial analysis capabilities, hydrological algorithms, and data. The main purpose is to overcome some of the main simplifications made in many modeling flood hydrographs, contributing to better simulate peak flow hydrographs for fixed return period (i.e., design flood). By leveraging geospatial analysis capabilities within a GIS framework, the tool uses spatially distributed data for a more accurate representation of basin characteristics and processes. This is particularly valuable for deriving probabilistic flood hydrographs, whose accurate predictions are essential for risk assessment and management, making the tool a valuable support in decision-making for hydrological agencies and practitioners. The tool has been tested on Sicilian catchments but given its open-source nature, modular, and flexible design, it is adaptable to different input data and geographic areas, proving a promising step forward in hydrological flood modeling.

1. Introduction

Design flood estimation is a pivotal process in the fields of hydrology and civil engineering; its use is needed to assess, in a probabilistic framework, the flood hydrograph magnitude, which in turn informs the planning, control and management of infrastructure, flood defenses and land. Its estimation process is, for these reasons, fundamental to the design of flood defenses, including dams, levees, spillways and stormwater systems. It ensures that these defenses can withstand extreme flood events while minimizing risks to communities and the environment. The design flood estimation methodology entails the integration of statistical analyses of historical rainfall data and watershed characteristics with the utilization of hydrological models, even with a simplified structure, to predict potential future flood magnitudes and frequencies.

About the role of hydrological models into design flood assessment, it is important to point out that they play a crucial role in understanding the intricate interactions between rainfall and runoff in a watershed, as well as in estimating the flow hydrograph features at a watershed outlet (Perez et al., 2015; Sahu et al., 2023; Wang et al., 2018). Specifically, hydrological models may be used for the simulation of specific hydrological processes, to predict the intensity and frequency of occurrence of extreme events such as floods and droughts (Agonafir et al., 2023; Gu et al., 2023; Ich et al., 2022; Meresa et al., 2023), or to assess the impact of future climate scenarios on the changes of water balance components (Brêda et al., 2020; Ich et al., 2022) and water resources management (Andrade et al., 2021; Nonki et al., 2023). With reference to hydraulic risk assessment, flood hydrographs estimated using hydrological models are critical for understanding the potential impacts of flooding on infrastructure, ecosystems, and communities. These hydrographs serve as inputs to hydraulic models, enabling the simulation of flood extent, water depth, and velocities. This process is essential for assessing hydraulic risk, identifying flood-prone areas, supporting flood zoning and management, and raising public awareness.

Due to the strong heterogeneity of basin characteristics and the complexity of processes, lumped models have often been preferred or used contextually to the spatially distributed ones (Moghadam et al., 2023; Nonki et al., 2023), especially in data-scarce environments. These models, in general, require less computational effort and parametrization, if compared to the semi-distributed and distributed ones, although they do not provide spatial insights of the process under study. However, in the latest years, this limit has been partially overcome thanks to the development of Geographic Information Systems (GIS) (Clark, 1998; Thakur et al., 2017; Velásquez et al., 2023), which has made it possible

* Corresponding author.
E-mail address: antonio.francipane@unipa.it (A. Francipane).

https://doi.org/10.1016/j.envsoft.2025.106497
Received 12 November 2024; Received in revised form 20 March 2025; Accepted 25 April 2025
Available online 30 April 2025

the integration of spatially distributed data and advanced analysis tools, leading to a more in-depth analysis of the streamflow response at the outlet of a watershed. The rapid worldwide deployment of GIS has been mainly driven by the increasing availability of spatial data, a growing number of computational resources, and the availability of different software products. Nowadays, a remarkable amount of data at different spatial and temporal scales (e.g., Digital Elevation Models - DEMs, land use/cover layers, stream network, meteorological data, etc.) and GIS-based software (e.g., QGIS, GRASS, GDAL, SAGA-GIS, etc.) are, most of the time, freely available, making it feasible to apply even hydrological semi-distributed or distributed models without excessive computational burden. Moreover, the increasing availability of geomorphological data and GIS tools has also facilitated the development of models aimed at simulating peak flow hydrographs (i.e., design flood) within a probabilistic framework at any given point in a basin.

Combining the TOPMODEL with GIS, Li and Zhang (2008) developed a GIS-based distributed hydrologic model where the watershed is divided into several subbasins. The runoff of every subbasin is calculated by the TOPMODEL, while the flow routing of each subbasin is calculated by means of a GIS-based isochrone curve method. Finally, the outflow process of each subbasin and the inflow of drainage network are routed by the Muskingum flow method to obtain the discharge hydrograph at the outlet of the watershed. Domniţa et al. (2010) developed a methodology to determine the surface runoff hydrograph in very small rural basins when the storm characteristics are known. The methodology was automated by implementing in a GIS framework four components that address the following requirements: the runoff depth, the runoff coefficient, the concentration time, and the discharge at a given point. Particularly, the discharge calculation is carried out by applying the rational method in each cell of the watershed to determine the specific discharge for that cell. Dang and Kumar (2017) used the hydrological model SCS TR-55 (Soil Conservation Service Technique Release 55) within a GIS framework to investigate rainfall-induced flood phenomenon in small sub-catchments. The model begins with a rainfall amount uniformly imposed on the watershed over a specified time distribution, which is converted to mass runoff by using the curve number (CN) method. Runoff is then transformed into a hydrograph by using unit hydrograph theory and routing procedures that depend on runoff travel time through segments of the watershed. Cho et al. (2018) proposed a hybrid hydrologic model to implement spatially distributed rainfall–runoff routing with the excess rainfall CN technique (SCS, 1957; 1972). The resulting model is a lumped conceptual and distributed feature model that focuses on flow simulations for a watershed outlet point (grid to point computation) rather than fully considering flow interactions between specified grid cells within the watershed (grid to grid computation).

Design flood analysis benefits from all the previous mentioned elements, such as hydrological models' ability to simulate watershed responses to rainfall, especially peak flows, GIS capabilities for managing spatially distributed data, and spatial analysis techniques that integrate detailed watershed characteristics into hydrological models, enhancing flood prediction reliability. However, developing a user-friendly GIS framework to generate design flood by combining all essential elements (e.g., data, models, and spatial analysis techniques) is not a trivial task.

One of the most challenging goals for these systems is to use simple models that, despite their simplicity, are still able to correctly model design floods by simulating the process of converting precipitation excess into runoff, which is routed downstream and combined to determine the total runoff hydrograph at a specific point in the drainage basin (e.g., the outlet of the basin). In most cases, the models use a transform method that relies on the concept of the unit hydrograph (UH; Sherman, 1932) relying on concepts such as the time of concentration and the time-area curve of a basin, for which the use of GIS may be a game-changing factor. This task is indeed not trivial and often difficult to solve, as it involves many factors such as the velocities at which water moves within the watershed, depending on whether the water flows along slopes or in the hydrographic network, as well as on land use, morphology, soil roughness, etc.

In this work we present a Python-based tool named GETAFLOOD (GEospatial Tool for Automatic derivation of design FLOOD), developed in open-source QGIS environment that integrates GIS functionalities, different open-source geospatial libraries, such as GDAL, SAGA, and WhiteboxTools (Lindsay, 2016), with hydrological modeling techniques. The aim of the work is to create an innovative framework that integrates data, existing hydrological algorithms/methods, and GIS functionalities to address two main aspects.

- providing a practical tool to enhance the hydrological flood modeling process for applications in hydraulic risk assessment, as well as in the design and management of hydraulic infrastructures;
- overcoming common simplifying assumptions in hydrological studies, such as those used to estimate the time of concentration and the time-area curve of a basin. In this regard, an improvement to the distributed unit hydrograph method has been developed and presented, although this is not the main target of the manuscript.

To the best of our knowledge, no existing framework in the current literature achieves these objectives. The tool derives the Depth-Duration-Frequency (DDF) curves following a regionalized procedure and derives the synthetic Chicago hyetographs for the given return periods. It also offers the chance to consider a climate change factor to account for the effects of current and future changes in climate on the DDFs. The flow hydrograph is lastly obtained by means of the joint application of the CN method, for the runoff depth estimation, and the distributed UH method based on a new algorithm specifically developed. One of the greatest advantages of the developed tool is that all these processes, which are typically performed separately by the user during the design flood analysis, are integrated into a single cascade workflow that includes also the data needed to achieve the scope. Once the user provides the necessary data outlined in Section 2.1.1, the tool simplifies the process, offering valuable support for people involved in design flood estimation.

The tool has been developed and tested in Sicily (Italy), proving to be a reliable and versatile tool in simulating peak flow hydrographs for both hydraulic risk planners, decision-makers and practitioners who are called to work in environments where few or no reliable measurements are available, especially those related to flow or runoff. One of the main advancements of the proposed tool, compared to methodologies previously applied in Sicily, is the assessment of a spatially distributed time of concentration layer, which makes it possible to derive a more realistic catchment response to precipitation. However, while we demonstrated the tool's functionality by applying it to our region (Sicily), it can be applied to any area of the world where the data outlined in Section 2.1.1 can be obtained and/or derived.

The paper is organized as follows. Section 2 describes the new plugin developed for QGIS. Section 3 introduces some use cases to test the ability of the tool in dealing with both historical and synthetic rainfall events. Finally, the results are discussed in Section 4, along with the main conclusions drawn from this study.

2. Methods

2.1. Overview of GETAFLOOD

The proposed tool follows a multistep framework that is based on four modules as summarized in Fig. 1: *i)* DATA imports spatial and temporal data needed to the tool; *ii)* GEO delineates the watershed for fixed outlet point and derives its morphometric characteristics and time of concentration; *iii)* RAIN uses rainfall forcings deriving from historical data or generates the design rainfall for a fixed return period and duration set equal to the concentration time of the basin and the subsequent hyetograph; *iv)* MODEL provides the flood hydrograph and is

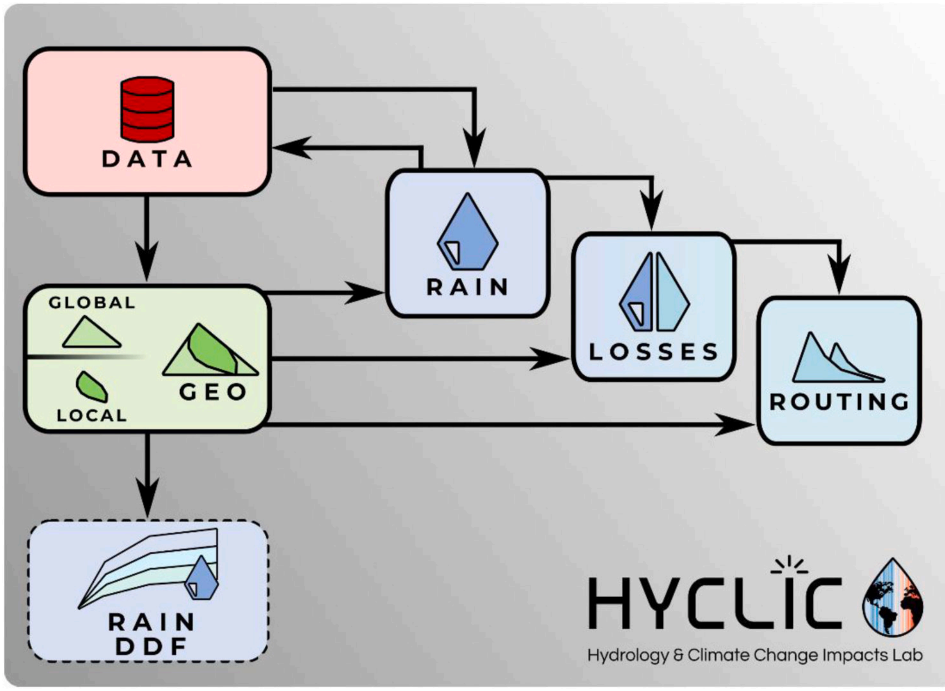

Fig. 1. GETAFLOOD multistep framework with mandatory (solid line) and optional (dashed line) modules.

composed by two submodules: MODEL-LOSSES, which calculates the net rainfall, and MODEL-ROUTING, which estimates the flood hydrograph at the outlet river section.

The tool also provides the opportunity to derive the Depth-Duration-Frequency (DDF) curves for a user-specified set of return periods (RAIN DDF module) or to simulate a historical flood event starting from observed rainfall data, if available. Based on the user's choice, the input data required by the tool may differ slightly, as will be specified in

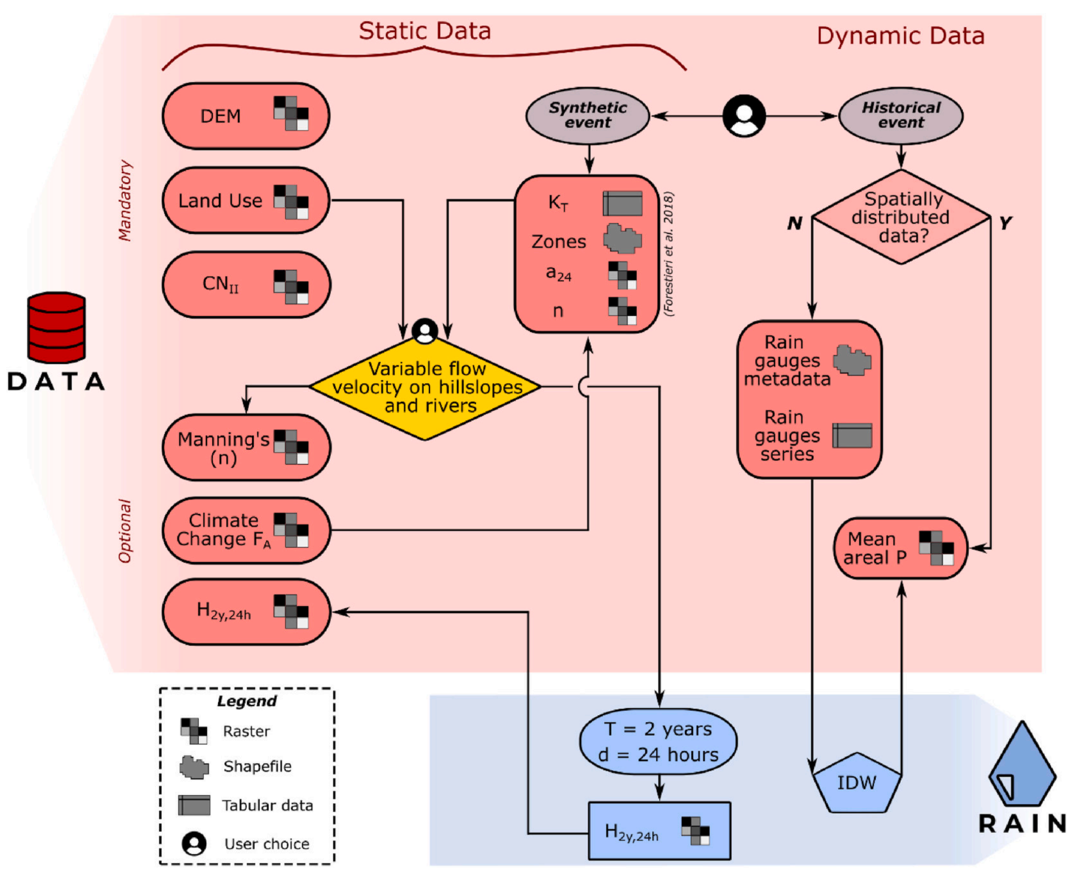

Fig. 2. – Schematization of DATA module.

Section 2.1.1. More details on each module will be provided below.

2.1.1. Module 1 – DATA: data preparation and import

To work properly, the tool requires various spatial (i.e., layers) and tabular (e.g., time series) data for the study area, which the user must prepare in advance. As introduced before, we will refer to the entire Region of Sicily. All data are stored in the DATA module, as shown in Fig. 2.

Starting with static data, the tool requires spatial layers including DEM, land use, CN_{II} and/or soil hydrologic groups (HSGs) as defined by the USDA-NRCS (2009), and the parameters needed for deriving the design rainfall (or the DDF curves) for a given return period. For Sicily, we used the regional frequency analysis (RFA) by Forestieri et al. (2018), which requires a layer related to the delineation of the homogeneous regions, and two layers for the a_{24}, and n parameters. Moreover, the tool requires a table (e.g., a.csv file) containing the dimensionless quantiles of the growth curves for each homogeneous region and different return periods (e.g., quantiles for return periods ranging from 2 to 500 years). When the user wants to reconstruct a historical flood event, some dynamic data are required. In particular, the spatio-temporal rainfall distribution during the event needs to be provided. If this information is not directly available, the user can enter the precipitation time series recorded by different rain gauges, together with their metadata. The attribute table of this last layer must contain a field named "id", where a unique code for each rain gauge station must be indicated. The same "id" code must be reported in the precipitation.csv file, containing the time series of precipitation observed at the considered rain gauges. The latter must be structured with a first column for the date (in the format dd/mm/yyyy), a second column for the time (in the format hh:mm), and subsequent columns for each station where recorded data are available. Fig. S1 in the supplementary material provides an example of the attribute table and the.csv file required to define the observed precipitation. In these cases, time series must have the same temporal resolution and duration. This information is necessary to spatially interpolate the precipitation time series using the IDW (Inverse Distance Weighting; Shepard, 1968) method and compute the mean areal precipitation time series for the area.

Depending on the option chosen to derive the time of concentration, the tool also requires raster layers for Manning's roughness coefficient, which can be obtained by reclassifying the land use layer (see Section 2.1.2 for more details), and the rainfall quantile for a 2-year return period and a 24-h duration, which can be calculated as the average intensity of a meteorological event with those characteristics, easily retrieved by the procedure implemented in the RAIN module (see Section 2.1.3 for more details). Additionally, for simulations of synthetic events, if the user wishes to account for the effects of ongoing climate change on precipitation quantiles, a raster layer of precipitation correction factors must be provided. For the tool to work properly, all layers must have the same coordinate reference system, although it is not necessary for the raster layers to have the same spatial resolution.

All data are imported into the tool by using the '*os.path*' module in Python 3 (Van Rossum and Drake, 2009) after the user specifies the path to the folder where the data are stored. It is strongly recommended to store spatial and tabular data in separate folders, and to further distinguish between folders for raster and vector spatial layers. The imported data are then used in the following modules to be corrected or obtain secondary input layers (GEO module), derive the rainfall forcing (RAIN module), or simulate the hydrological processes (MODELS module). For more details, see Sections 2.1.2 through 2.1.4. Table S1 in the supplementary material summarizes all the data necessary for properly running the tool, distinguished by type.

2.1.2. Module 2 – GEO: geomorphological analysis

The main objective of this module is to process data imported from the DATA module to create additional spatial and tabular input data for the derivation of hydrographs.

The GEO module is divided into two sub-modules: GEO-GLOBAL and GEO-LOCAL (Fig. 3). The first sub-module operates on the entire study area to generate secondary input data layers (e.g., slope, flow directions, stream network, isochrones). These layers are then used in the GEO-LOCAL sub-module to delineate the basin and determine its characteristics (e.g., boundaries, time-area curve, concentration time, geomorphological parameters etc.). Basin information is subsequently used in both the RAIN and MODEL modules to derive the hydrograph in response to a historical or synthetic precipitation event. The GEO-GLOBAL sub-module typically needs to be run only once. However, this does not prevent the user from running the entire GEO module as needed; this could happen when conditions change or when the tool is used in different areas.

2.1.2.1. GEO-GLOBAL. The GEO-GLOBAL begins by processing the DEM to identify and fill any depressions and flat areas that would otherwise impede water flow to neighboring cells, using the '*Fill Depressions* Wang and Liu (2006) algorithm from WhiteboxTools library. After correcting the DEM, the slope, flow direction, and flow accumulation layers are derived in a cascading process using the '*Slope*' (Florinsky, 2016), '*D8Pointer*' (O'Callaghan and Mark, 1984), '*D8FlowAccumulation*' (O'Callaghan and Mark, 1984) algorithms from WhiteboxTools library, respectively. The flow accumulation layer is then used to extract the hydrographic network by applying a threshold value; cells with a flow accumulation higher than the threshold are classified as network cells, while all others are classified as hillslope cells. After various attempts, the threshold was set equal to 10,000 cells, which allows for a more accurate reproduction of the hydrograph network at the spatial scale of 1:10,000, as used to represent the stream network of Sicily in the SITR (*Sistema Informativo Territoriale Regionale* – Regional Geographic Information System) geoportal (https://www.sitr.regione.sicilia.it/geoportale/).

At this stage, one of the most delicate phases of the GEO-GLOBAL sub-module begins: the determination of the isochrone layer (Fig. 3), which represent the spatial distribution of travel time of a cell, defined here as the time it takes for a generic raindrop that falls on that cell to reach the basin's outlet, always flowing on the surface. The spatial distribution of travel time allows for deriving both the time-area curve of a basin, which is a fundamental input for the kinematic model, and the time of concentration, which is the time it takes a drop of water to travel from the most distant point in the basin to the outlet, represented by the maximum value of such distribution. Despite being a fundamental parameter in numerous contemporary hydrological models embraced by both professional and scientific communities, a unique approach to evaluate the time of concentration of a basin is still missing (Evangelista et al., 2023) and empirical formulations (e.g., Giandotti, 1933; Kirpich, 1940; SCS; etc.) are generally used (Salimi et al., 2017). These formulations have many limitations. For instance, most of them were developed several decades ago, considering basins located in specific regions of the world. Also, information on their technical foundations is often limited, as well as the nature and number of observed flood events used in their calibration (Grimaldi et al., 2012a). Moreover, they only provide the maximum time of concentration of the basin, while some hydrological applications require the spatial distribution of the travel times. Finally, these formulations are designed to be applied between specific ranges of basin size, slope, or other morphometric characteristics, whereas they are often applied indiscriminately. Over the years, many studies have tried to point this problem out by highlighting the differences in the results when different formulations are used on the same watersheds (e.g., Fang et al., 2008; Grimaldi et al., 2012a; Almeida et al., 2015; Michailidi et al., 2018; González-Álvarez et al., 2020). Since no single method for estimating response times is universally superior, given the diverse range of climatological, geomorphological, and hydrological conditions encountered in practice, Evangelista et al. (2023) sought to establish analytical relationships between velocities and basin

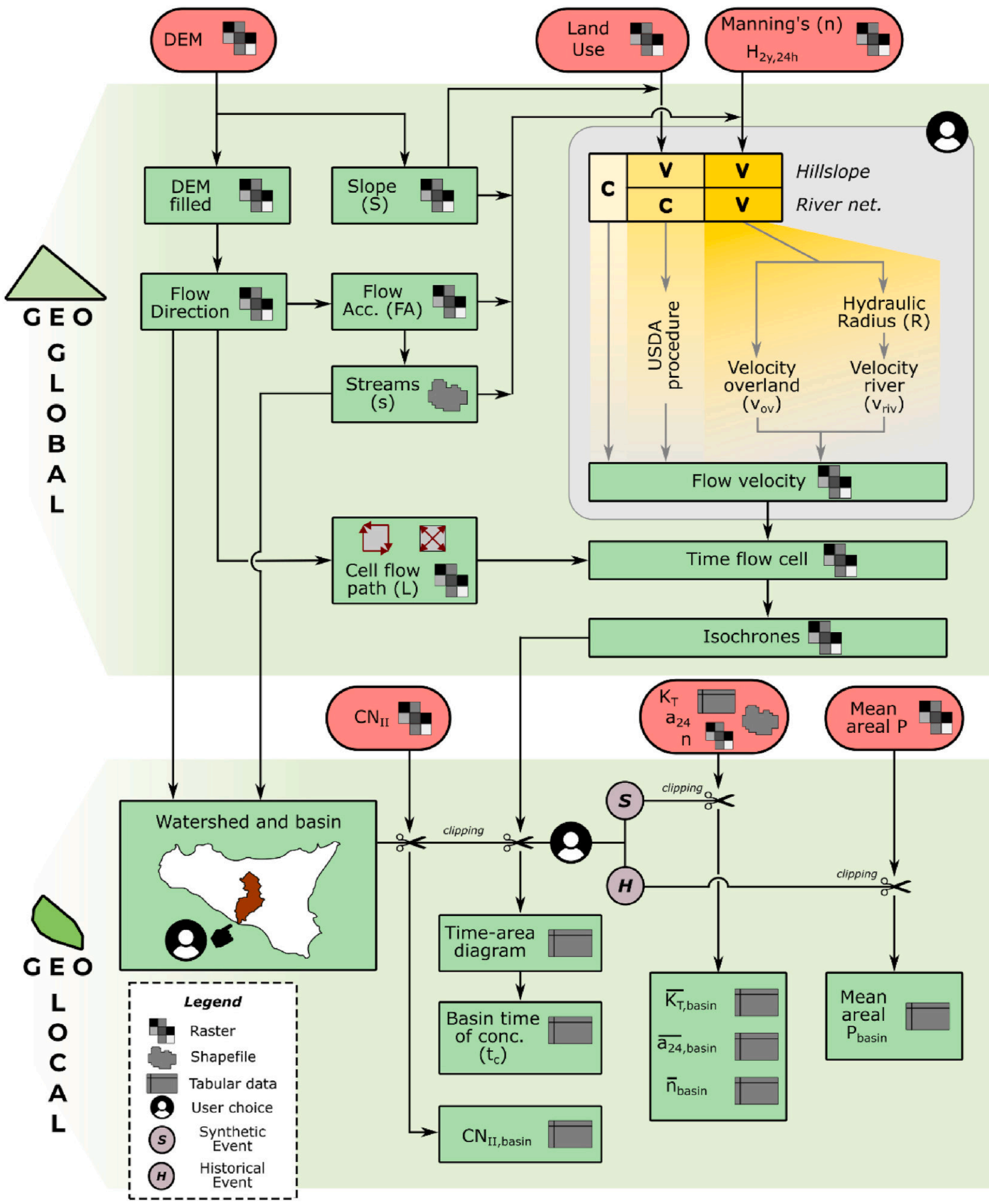

Fig. 3. Flowchart of GEO (GLOBAL and LOCAL) module.

morphological features. These relationships aim to serve as practical tools for calibrating new formulas, offering concrete guidance to practitioners, and proposing a methodology for identifying robust formulas based on observed velocities rather than observed response times.

A good estimate of the concentration and travel times of a basin, along with its time-area curve, must necessarily involve the most accurate definition of the velocities at which water flows within the watershed. This is, undoubtedly, the most critical step of this phase. Indeed, transfer velocities along slopes and in the hydrographic network vary significantly and can depend on different factors. Noto and La Loggia (2007), for example, presented an approach for predicting streamflow at a watershed outlet that accounted for variations in velocity between hillslopes and the stream network, although it required the calibration of two coefficients to define the velocity field across the watershed. Michailidi et al. (2018) implemented a simplified velocity approach in a GIS environment, using easily retrieved geographical data from many basins of diverse sizes and shapes in Italy, Greece, and Cyprus to establish regional formulas as functions of key geomorphological characteristics of the catchment and the main watercourse.

To address this issue, the tool offers the user three different options: 1) using a constant flow velocity across the watershed, 2) using variable flow velocities for the hillslopes as a function of slope and land use, but a constant velocity for the network, or 3) using a spatial distribution of flow velocity across the entire watershed based on its morphometric characteristics. Specifically, for the last option, an *ad hoc* method has been developed according to Cho et al. (2018), which will be explained in the following section (i.e., option 3).

Once the flow velocity is fixed (i.e., option 1) or the spatial distribution of flow velocities is derived for each cell (i.e., options 2 and 3), the cell travel time layer can be obtained by dividing the path length by the flow velocity in each cell and accumulating the result along the flow directions using the '*Maximum Flow Path Length*' tool from the SAGA library. In this case, the path length in each cell is assumed equal to the cell size, *l*, if the movement occurs along one of the main cardinal directions, or equal to $l\sqrt{2}$ if it occurs along one of the diagonal directions. The travel time layer also allows for determining the time of concentration of the watershed by considering the highest value in the travel time layer.

2.1.2.2. Option 1 – Constant flow velocity across the watershed. This is the simplest option available to define the flow velocity across the basin, as it assumes that each cell in the watershed is characterized by a constant flow velocity, which is defined by the user based on their experience. Previous studies suggest using a constant flow velocity in the range of 0.02–2.0 m/s across the watershed (Grimaldi et al., 2010, 2012a).

2.1.2.3. Option 2 – Variable flow velocity across hillslopes and constant flow velocity in the river network. This option uses different flow velocities depending on whether the watershed cell is a hillslope or part of the river network. For hillslope cells, the flow velocity can be set according to the procedure developed by the U.S. Department of Agriculture Soil Conservation Service (1986), which provides flow velocity in a cell based on its slope and land use information (Fig. S2 in the supplementary material). For each land use class, LU_i, defined by the Corine Land Cover project (Buchhorn et al., 2020; https://land.copernicus.eu/en/products/corine-land-cover) and derived from the DATA module, a lookup table provides the velocity, v_{LU_i}, as a function of the slope, S, and two parameters, a_{LU_i} and b_{LU_i}, as follows:

$$v_{LU_i} = a_{LU_i} S^{b_{LU_i}} \tag{1}$$

For river network cells, following Noto and La Loggia (2007), the user can define a constant flow velocity within the range 0.5–2 m/s.

2.1.2.4. Option 3 – Variable flow velocity across the watershed. In this case, the tool derives the spatial distribution of flow velocities across the watershed using two different approaches for hillslopes and the river network. Starting from the layers of slope, land use, and rainfall quantile for a 2-year return period and a 24-h duration stored in the DATA module, the transfer velocity along hillslopes, $v_{hillslope}$, can be expressed using the Manning equation, according to Cho et al. (2018), as follows:

$$v_{hillslope} = \frac{(iL)^{0.4} S^{0.3}}{419,28\, n^{0.6}}, \tag{2}$$

where i [mm/h] is the intensity of the rainfall event over the basin, L [m] is the length of flow paths in the cell, S [m/m] is the slope, and n [-] is the Manning's roughness coefficient. Using a raster geometry, L can be assumed equal to the cell size if the flow moves along one of the main cardinal directions, or equal to $L\cdot\sqrt{2}$ if it moves along one of the two diagonal directions.

Regarding the flow in the channel, the Manning equation can be modified as follows:

$$v_{channel} = \frac{1}{n} R^{\frac{2}{3}} S^{\frac{1}{2}}, \tag{3}$$

where R [m] is the hydraulic radius of the channel section, which is function of the section's geometry and wetted perimeter, while n [-] and S [m/m] are the Manning coefficient and the slope of the channel, respectively.

The most uncertain part in deriving the flow velocity layer concerns the estimation of the hydraulic radius. Here, we suggest estimating it from the flow accumulation layer following the procedure described in Liu et al. (2003). According to this approach, for each cell of the calculation domain, the hydraulic radius, R, is expressed as a function of the flow accumulation, FA, according to the following power relationship:

$$R = a(FA)^b, \tag{4}$$

where a and b are estimated, for a fixed return period, based on the minimum and maximum values that the hydraulic radius can assume when considering the area drained by a single cell and the area drained by the entire basin, respectively. Following Liu et al. (2003), we considered a 2-year return period, which the authors regard as representative for normal floods, with corresponding optimal values of $a =$ 0.1 and $b = 0.5$. These values yield channel and hillslopes velocities that are consistent with typical values for Sicilian basins. As suggested by Liu et al. (2003), the return period should be increased when considering more extreme flood events.

Specifically, the Manning's roughness coefficient layer was obtained by reclassifying the land use layer provided by the Copernicus Global Land Service (https://land.copernicus.eu/global/products/lc) stored in the DATA module. The layer of the intensity of precipitation, i, impacting the watershed (see equation (2)) was expressed as the average intensity of a meteorological event with a return period of 2 years and a duration of 24 h according to Liu et al. (2003). This can be easily retrieved using the regionalization procedure by Forestieri et al. (2018) implemented in the RAIN module (see Section 2.1.3 for more details). The tool stores the Manning's roughness coefficient and the precipitation intensity layers in the DATA module, saving time in the case of future applications for the same area.

2.1.2.5. GEO-LOCAL. Once the GEO-GLOBAL sub-module has completed all its operations, the tool will display the hydrographic network layer on the screen. The user is then prompted to identify the basin's outlet by left-clicking on the desired point within the hydrographic network. Once the basin's outlet is defined, the tool will use the '*Watershed*' tool from the Whitebox Tools to delineate the watershed. This tool only requires the layer of flow directions, which has been calculated in the GEO-GLOBAL module, and the outlet point. The raster of the watershed is then converted into a polygon, which serves as a mask to clip all layers necessary in subsequent processes (e.g., travel time, flow directions, stream map, CN, layers needed for the regionalization by Forestieri et al. (2018) or the mean areal precipitation maps if the tool is used to simulate an historical flood event). In particular, the tool uses the '*Clip Raster by Mask Layer*' algorithm from the GDAL library, if the layer is a raster, and the '*Clip*' tool from the Whitebox Tools, if the layer is a vector. The tool also calculates key watershed characteristics, such as its area, time of concentration, time–area curve, and spatial average CN value. Specifically, the time–area curve is obtained by dividing the travel time layer obtained in the GEO-GLOBAL sub-module into isochronal lines and, for each of them, evaluating the fraction of the basin area that contributes to surface runoff at the outlet section within the specified time interval; this curve shape influences both the shape of the hydrograph and the magnitude of its peak at the basin's outlet section.

2.1.3. Module 3 – RAIN: rainfall forcing preparation

The RAIN module (Fig. 4) is used to create the forcing hyetograph required for deriving hydrographs in both historical and synthetic cases. Additionally, the module provides the rainfall quantile layer for a 2-year return period and a 24-h duration across the entire study area, as mentioned in Section 2.1.1.

The module operates and interacts with all the other modules differently, depending on whether the tool must be applied to simulate the response to synthetic or historical precipitation. For the synthetic case, the tool computes the design rainfall considering a user-specified return period and the critical duration, d_{cr}, retrieved from the GEO module.

The tool also provides a stand-alone option to derive the DDF curves for several user-specified return periods according to the regionalized procedure proposed by Forestieri et al. (2018) for Sicily, which is summarized in Fig. S3 in the supplementary material. To do this, the RAIN DDF module uses the characteristic (average) values for the entire basin for the parameters a_{24} and n, along with the homogeneous region

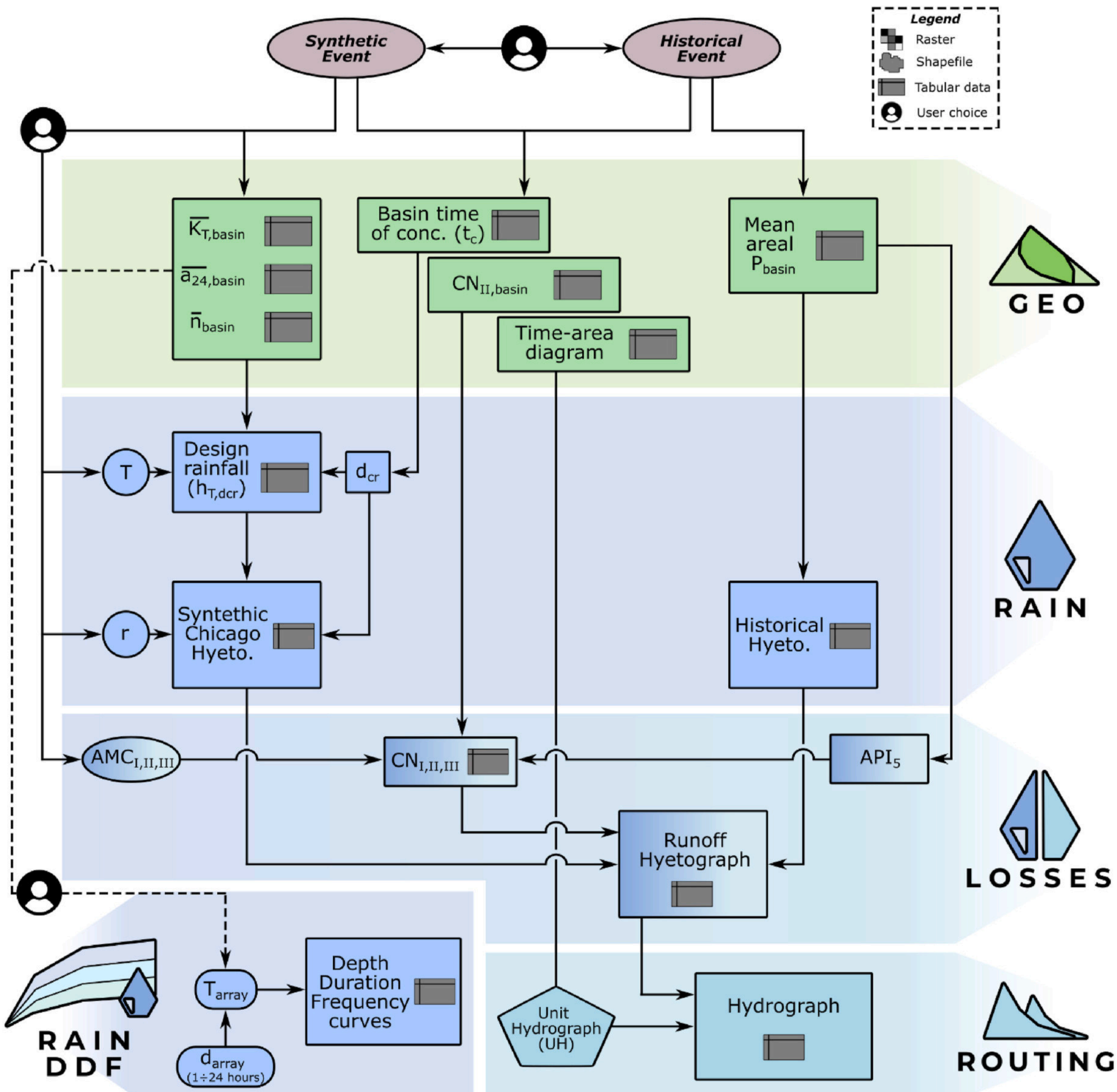

Fig. 4. Flowchart of RAIN, LOSSES AND ROUTING modules, together with the optional module to compute the Depth-Duration-Frequency curves (RAIN DDF).

(s) where the watershed lies. The DDF curves are finally computed and shown for all the durations between 1 h and 24 h.

According to the regional analysis by Forestieri et al. (2018), the maximum precipitation depth, $h_{d,T}$, for a given duration, d, and return period, T, at a site belonging to a region r is obtained from the product:

$$h_{d,T} = h_r(T) \cdot \mu(d) \tag{5}$$

where $h_r(T)$ is a dimensionless variable and $\mu(d)$ is a *scaling factor*. The assumption underlying this method is that there exist regions r that can be labeled as homogeneous since they can be identified by a single frequency distribution law of the variable $h_r(T)$, called "*growth curve*". For each homogeneous region and for different return periods, T, the authors provide the values of $h_r(T)$ and the equation to determine the values of $h_r(T)$ for the return periods not explicitly tabulated. To estimate $\mu(d)$ at a site, the following model can be adopted:

$$\mu_S(d) = a_{24} \cdot \left(\frac{d}{24}\right)^n \tag{6}$$

where the parameters a_{24}, representing the median of extreme precipitation depth for a duration of 24 h, and n are provided by means of two raster layers that enable estimation of these parameters at any site within the region. For more details about the regional study, see Forestieri et al. (2018).

The potential effects of ongoing climate changes on the definition of the precipitation quantile are accounted for by applying a climate change factor, F_A, that is the one from Treppiedi et al. (2024a, b) in the case of Sicily (Fig. S3 in the supplementary material), or any multiplicative layer for other study areas (Martel et al., 2021).

Once the design rainfall (or the mean areal precipitation for the historical event, see Section 2.1.1) is computed, the design hyetograph is generated using the Chicago hyetograph method (Keifer and Chu, 1957), considering one or more user-defined peak position, r, and a duration equal to the concentration time of the watershed, d_{cr} (see GEO module). The temporal discretization of the hyetograph depends on the concentration time of the basin, with a time step of 0.5 h for $d_{cr} < 3h$, and a time step of 1 h for $d_{cr} \geq 3h$.

2.1.4. Module 4 – MODELS

The last module consists of two sub-modules, namely LOSSES and ROUTING (Fig. 4). The LOSSES sub-module calculates the losses in precipitation to determine the surface runoff at any point within the basin, while the ROUTING sub-module handles the subsequent downstream routing and combination of runoff to determine the total runoff hydrograph at a specific point in the drainage network. The two sub-modules will be explained in detail in the following.

2.1.4.1. MODEL-LOSSES. For the calculation of the losses in precipitation, the tool offers two different options: the SCS-CN method, originally developed by the Soil Conservation Service (1957; 1972), and the Horton model (Horton, 1933, 1938). Both methods depend on the soil characteristics expressed through soil hydrologic groups (HSGs) as defined by the USDA-NRCS (2009).

The SCS-CN method, in its final formulation, assumes that the specific volume of surface runoff, Q, can be calculated as:

$$Q = \frac{(P - I_a)^2}{P - I_a + S}, \tag{7}$$

where P is the specific volume of rainfall, I_a is the initial abstraction, and S is a specific volume that characterizes the maximum potential retention of the soil. The parameter S in equation (7) depends on the dimensionless parameter CN, which ranges between 0 and 100, where higher values indicate less permeable soils, linked to S by the relation $S = 254(100/CN - 1)$.

The other parameter to estimate for determining Q is I_a, which represents the specific volume of rainfall subtracted a priori from the water balance. Experimental data indicate that this parameter is always proportional to S, thus it has been established to set it equal to cS, with c usually equal to 0.2 (SCS, 1972). In this case, c has been set to 0.2, but it can be adjusted to calibrate the model.

The CN value depends on several factors, including soil moisture conditions prior to the rainfall event, which are evaluated in relation to the Antecedent Moisture Condition (AMC). The AMC is obtained by comparing the antecedent precipitation index (API - Mishra and Singh, 2013) for the five days prior (API_5) to the flood event, which is the total rainfall fallen during that period, with some threshold values that vary depending on the season as tabulated by the Soil Conservation Service (1957; 1972). The SCS-CN procedure requires the CN to be calculated based on average soil moisture conditions (i.e., CN_{II}), which may be reduced or increased using equations provided by the Soil Conservation Service (1957; 1972). For synthetic precipitation, the AMC is defined by the user, who can choose to work with more than one AMC condition at the same time. For historical events, instead, the tool calculates the API_5 to determine the AMC and, therefore, selects the appropriate CN value to use. If the recorded event lasts less than 5 days and/or there is no information about the pre-event precipitation, the user can manually specify an AMC value, as for the synthetic case.

The tool models the surface runoff using the CN_{II} layer that is retrieved by the DATA module. Since the CN primarily depends on the combination of the soil type and the land use/cover, which can change significantly over time, we updated the CN_{II} layer for Sicily using the most recent land use data available and a highly detailed, up-to-date soil database (see Section 3.2 for more details).

The development of the updated CN_{II} layer required defining the hydrological soil groups (HSGs) for Sicilian soils. Following the classification proposed by the USDA-NRCS (2009), the soils were classified as A, B, C, and D. The HSG layer, available in the DATA module, can be used to run the LOSSES sub-module using the Horton model, which is an empirical formula typically expressed as a function of time:

$$f = f_c + (f_0 - f_c)e^{-kt}, \tag{9}$$

where f_0 is the initial infiltration rate (mm/h) when the precipitation starts, f_c is the final infiltration rate (mm/h) when the soil is saturated, and k is a decay constant (1/h) that expresses the rate at which the infiltration capacity decreases with time t. The values of the three Horton's infiltration model parameters, which depend on soil characteristics, can be found in the literature as a function of HSGs and are reported in a look-up table in DATA module.

Regardless of the method used, the resulting net hyetograph or surface runoff will be used in the ROUTING sub-module to generate the flood hydrograph at the outlet.

2.1.4.2. MODEL-ROUTING. As previously mentioned, the ROUTING sub-module routes and combines surface runoff to obtain the hydrograph at a given point. The sub-module relies on the concept of the unit hydrograph (UH), which represents the basin's outflow resulting from one unit of direct runoff generated uniformly over the drainage area at a consistent rainfall rate during a specified rainfall duration (Shepard, 1968). Generally, the UH model attempts to relate the parameters of a parametric UH model to watershed characteristics. The fundamental concept of the UH is that the runoff process is linear, meaning that amounts greater or less than one unit is simply a multiple of the unit hydrograph.

Already in the 1990s, Maidment (1993) derived a GIS-based time--area diagram assuming a spatially variable but time-invariant flow velocity field, developing a UH based on the incremental areas (isochrones) of the time-area diagram under the assumption of a pure translation process. In a subsequent study, Maidment et al. (1996) presented a more sophisticated flow model that incorporated both translation and storage effects in the watershed, enabling the consideration of upstream drainage areas to define a local velocity function for each cell. In the same years, Rodríguez-Iturbe and Rinaldo (1997) proposed the width function formulation of the geomorphological instantaneous unit hydrograph (GIUH). This method used the width function, which is the number of sites at the same distance from the outlet, as measured along the streams and the drainage path, to derive the concept of isochrones under the hypothesis of constant velocities throughout the network. In the 2000s, further studies on GIS-based spatially distributed UH methods for runoff routing introduced new algorithms for the width function (Grimaldi et al., 2012b) and time-area curve computation based on watershed morphology and land use (Noto and La Loggia, 2007).

In this case, the UH relies on the time-area curve and the concentration time of the basin, which were obtained in the GEO-LOCAL sub-module (see Section 2.1.2). Starting from the time-area curve and applying the principle of superposition of effects, it is possible to derive the flood hydrograph of the basin through a convolution operation between the precipitation and the vector of isochronal areas. According to this operation, the discharge, q_k, at time $t = k \cdot \Delta t$ is obtained from the sum of contributions due to rain occurring before that time; if U_{k-j+1} is the value of the UH for $t = (k - j + 1) \cdot \Delta t$, the flood hydrograph per unit area at the outlet section can then be written, in discrete terms, as:

$$q_k = \sum_{j=1}^{k \le m} P_j U_{k-j+1} \Delta t \tag{10}$$

where P_j indicates the net rainfall volume at time j, m and n indicate the number of ordinates of the UH and P, respectively, and $k = n + m - 1$.; the flow hydrograph, Q_k, is obtained by multiplying q_k by the basin area, A.

2.2. The QGIS plugin

The GETAFLOOD is developed as a QGIS plugin program written in Python 3 (Van Rossum and Drake, 2009). The purpose of the plugin is to provide a user-friendly interface to prepare input data, configuring simulation settings, and viewing, analyzing, and post-processing results in QGIS.

To make the tool work correctly, QGIS3 (https://download.qgis.org) is required on the system. In particular, the tool was developed and tested with the long-term release (LTR) version of QGIS3 Prizren

(3.34.7). After QGIS installation, the tool can be installed from an installer file (Getaflood.exe) by onetime manual activation via the “Manage and Install Plugins” window under the “Plugins” menu in QGIS (points 1 and 2 in Fig. 5). The plugin can be then launched from the “Plugins” menu (point 3 in Fig. 5) or from the QGIS toolbar (point 4 in Fig. 5). Users are required to install also the WhiteboxTools library (Lindsay, 2016) for hydrological modeling operations.

The interface of the tool is made of three main modules: *Input layers for Sicily and paths where to save results for the basin*, *Hyetograph type*, and *Other parameters* (Fig. 6a). In particular, the first module is implemented in three different tabs: *Precipitation parameters* (Fig. 6a), *Hydrological parameters* (Fig. 6b), and *Paths to save outputs* (Fig. 6c).

The *Precipitation parameters* tab (Fig. 6a) allows the user to input the vector layer of the homogeneous regions and the raster layers of parameters a_{24}, n, and $h_r(T)$ of the regionalization developed for Sicily by Forestieri et al. (2018). To make the tool even more versatile for other areas, future releases will take into account the possibility of considering RFAs with different parameters or spatial maps of quantiles retrieved with simpler methods.

The *Hydrological parameters* tab (Fig. 6b) allows the user to input the raster layers of curve number, flow directions, stream network, and isochrones. As specified in the tab, the last three layers have been derived for the entire Sicily following the procedure developed by Cho et al. (2018) and described in Section 2.1.2 (see Fig. 3).

The *Paths to save outputs* tab (Fig. 6c) allows the user to specify the paths of the folders where to save the outputs of the plugin distinguished by output type (i.e., raster, vector, table, and image).

The *Hyetograph type* module (Fig. 6a) makes it possible to define the type of simulation that the user wants to run, i.e., run the hydrological response to a synthetic event defined by means of a DDF curve or to a historical rainfall event that occurred in the past by means of observed precipitation time series recorded at different rain gauge stations. In the last case, the position of stations and rainfall time series at each station must be specified in the fields “Rain gauges (only for historical case)” and “Rainfall time series (only for historical case)”, respectively. Only for the synthetic case, the user has the chance to consider the effects of climate change on the definition of the DDF and, consequently, of the project hyetograph.

Finally, the *Other parameters* module (Fig. 6a) allows the user to define some other parameters, such as specifying one or more return periods for calculating the DDF curves, one or more peak positions to define the Chicago hyetograph, one or more AMCs for runoff calculation. It also allows for considering a percentile of the concentration times to calculate the concentration time of the basin. This last makes it possible to exclude some singularity points that are characterized by very high concentration times (e.g., flat areas) and that would make the concentration time of the basin unrealistic.

3. Use cases and datasets

The plugin has been developed and tested for the entire island of Sicily and it currently works for this region, though it can easily be extended to other areas of the globe.

This section presents firstly the datasets used to develop and run the

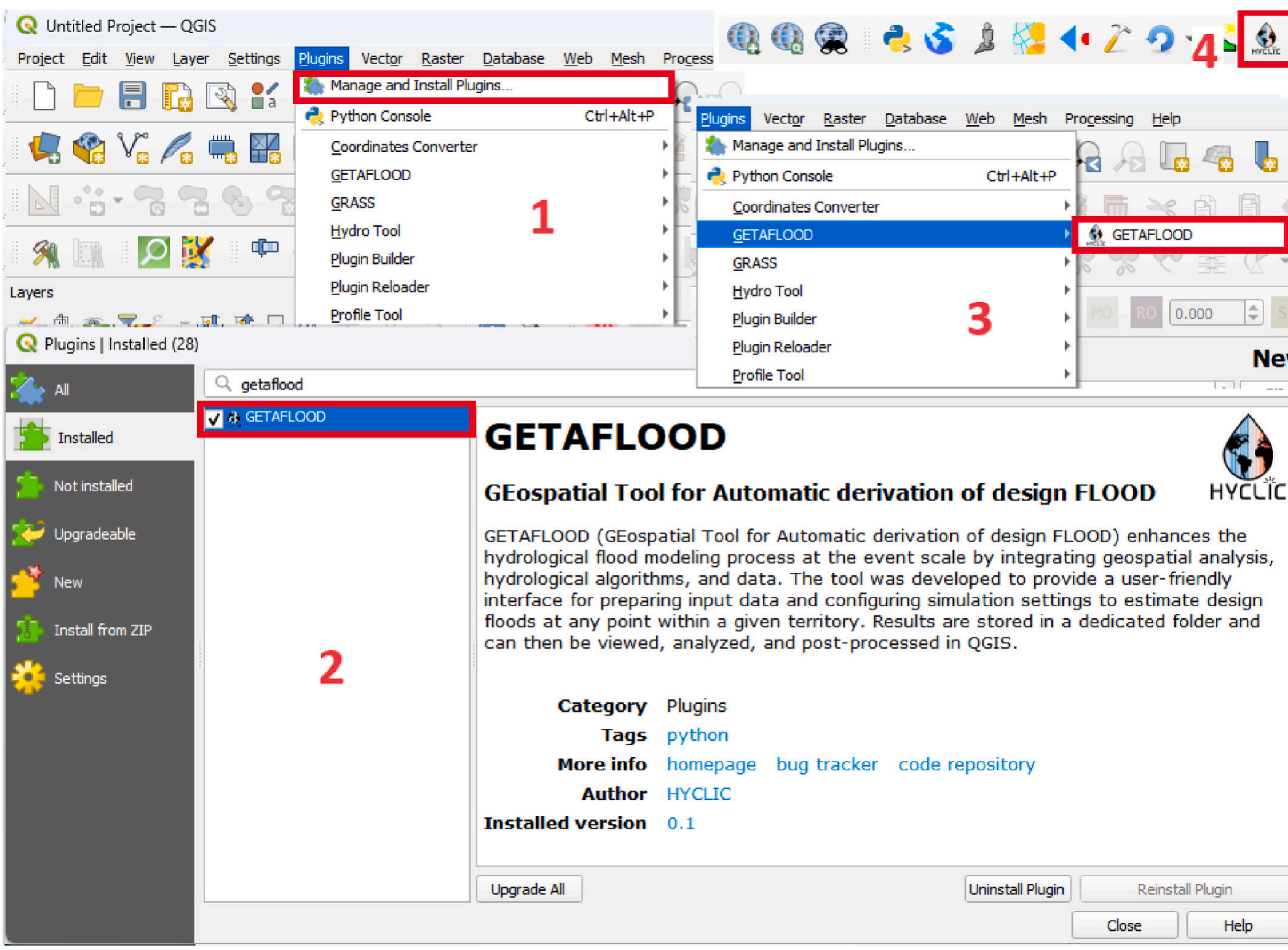

Fig. 5. GETAFLOOD installation and activation in QGIS.

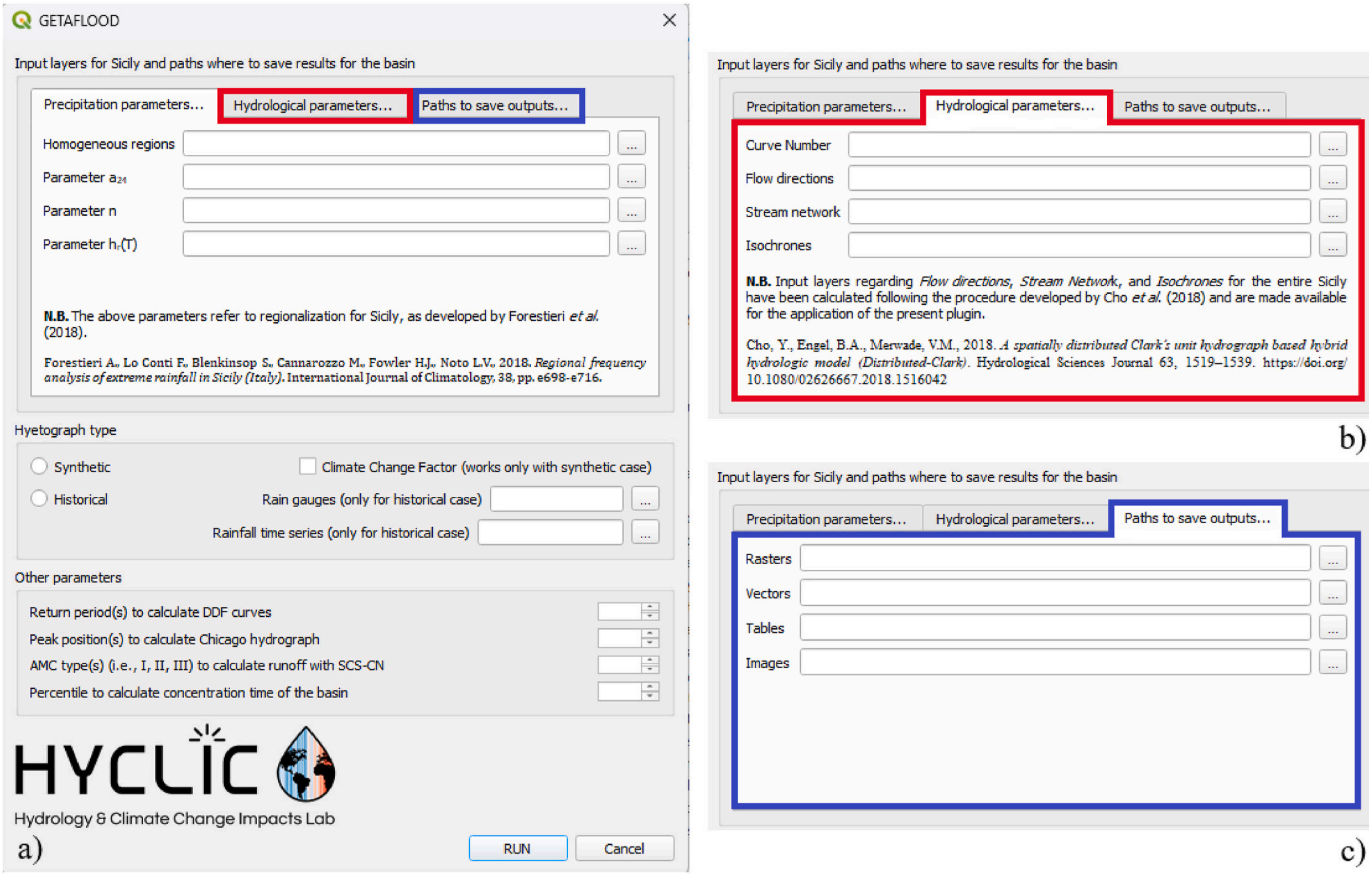

Fig. 6. Main interface of the GETAFLOOD with zooms on a) input section for *precipitation*, *hydrograph*, and *other parameters*, and the definition of b) *hydrological parameters*, and c) *output paths*.

plugin at a regional scale and then the use cases proposed to demonstrate aspects of the developed methodology, namely.

1. Calibration of the methodology for three Sicilian basins of different size using historical data;
2. Run of a synthetic case for the Oreto basin.

3.1. Climate dataset

For the calibration and the run of the plugin, the user can use precipitation data coming from any available rain gauge network, so long as the user has the position of the rain gauge stations and the time series of precipitation recorded in those stations.

In this study we used data of precipitation and discharge collected from the *Autorità di Bacino della Regione Sicilia* (i.e., Basin Authority of the Sicilian Region, hereinafter referred to as AdB), which managed historical stations installed across Sicily from the 1940s until a couple of years ago. AdB monitoring network, whose number of functioning stations is variable over time, included ~200 tipping-bucket rain gauges and as many stream-gauges. Data are retrieved with a time resolution of 10 or 30 min, even though time series are often incomplete.

3.2. DEM, curve number, soil, and land use datasets

The DEM for Sicily was obtained from the TINITALY DEM version 1.1, which covers the whole Italian territory and is developed by the *Istituto Nazionale di Geofisica e Vulcanologia* (i.e., National Institute of Geophysics and Volcanology, hereinafter referred to as INGV) in GeoTIFF format, the UTM WGS 84 zone 32 projection system, and a spatial resolution of 10 m (Tarquini et al., 2007; https://tinitaly.pi.ingv.it/).

The curve number (CN) layer for the entire Sicily was obtained by intersecting the raster layer of hydrological soil groups (HSGs) with that of the land use/cover coming from the Corine Land Cover project (Buchhorn et al., 2020; https://land.copernicus.eu/en/products/corine-land-cover) according to USDA-NRCS (2009). The layer of the CN was obtained by using the soil information coming from an updated database of Sicilian soils provided by the *Consiglio per la Ricerca in Agricoltura e l'Analisi dell'Economia Agraria* (CREA). CREA realized the geometric and alphanumeric database of the Italian soil regions (Righini et al., 2001) and published the guidelines of the methods for soil survey and data informatization (Costantini, 2007) with the attached developed management software CNCP 3.0, for the collection and analysis of database of pedological information (L'Abate et al., 2007).

3.3. Use cases basins: the Oreto, Pollina, and Platani river basins

The procedure outlined in the previous sections has been tested on three different Sicilian basins characterized by different extensions, shown in Fig. 7, to test the ability of GETAFLOOD tool to simulate the hydrological response to both synthetic and historical precipitation.

The Oreto at Ponte Parco catchment has an extension of about 70 km^2 and an elevation ranging between about 125 and 1310 m a.s.l. with a mean slope of about 18°. It is located upstream of the city of Palermo. The Pollina at Ponte Vecchio catchment extends for about 100 km^2, with elevations ranging between about 200 and 1950 m a.s.l. and a mean slope of 19.5°. The Platani at Passofonduto catchment is the largest of the three basins considered here and develops in the central part of the island, covering an area of about 1400 km^2, with elevations ranging from approximately 140 to 1550 m a.s.l. and a mean slope of 12°. The

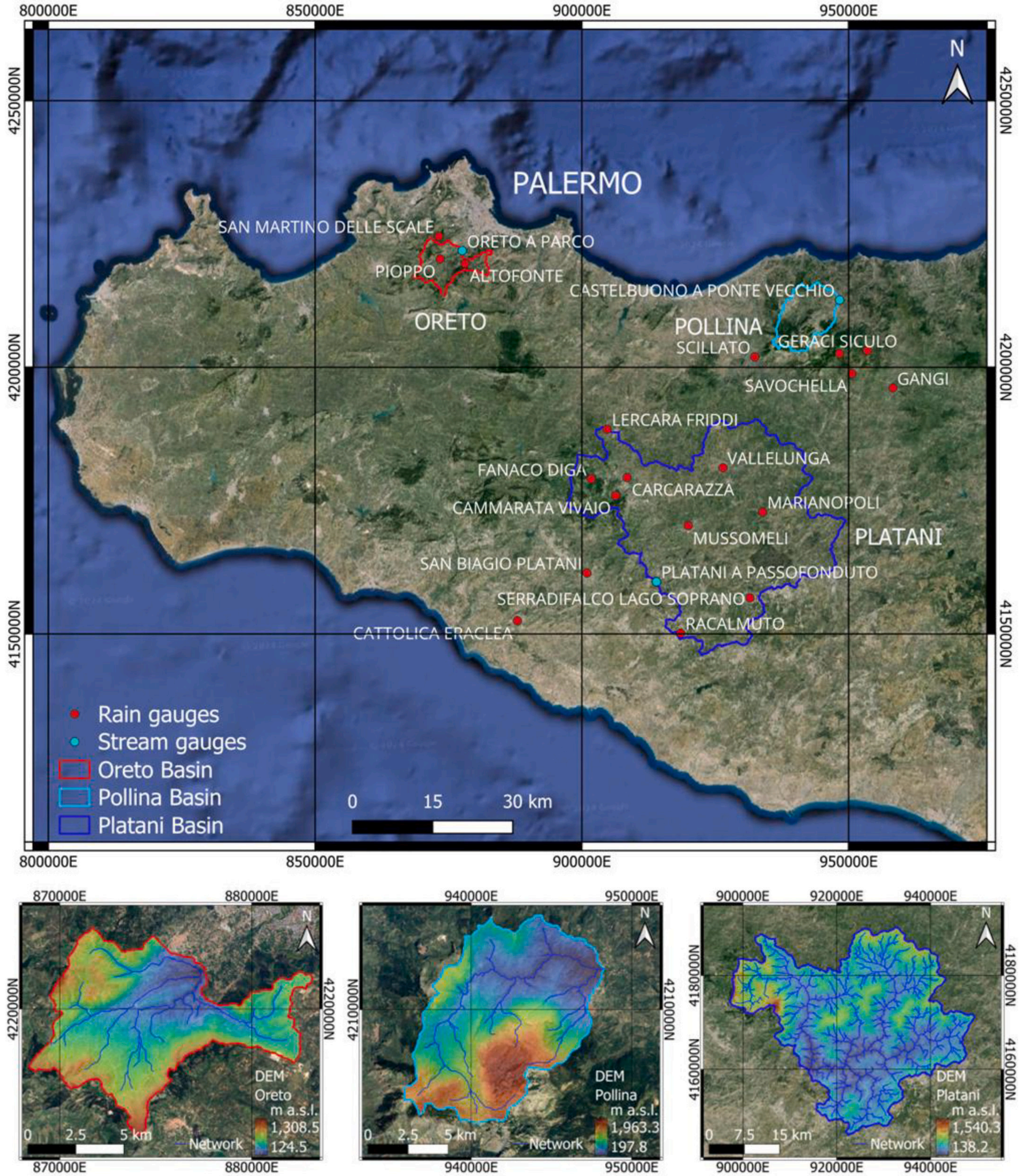

Fig. 7. Aerial view and DEMs of the Sicilian basins of the Oreto at Ponte Parco, Pollina at Ponte Vecchio, and Platani at Passofonduto. Red and cyan points indicate the rain and stream gauge stations, respectively, used for the calibration of the modeling framework here developed. (For interpretation of the references to colour in this figure legend, the reader is referred to the Web version of this article.)

rain and stream gauges used in this study are shown in Fig. 7 as red and cyan points, respectively. Additional information about the three previously mentioned basins is provided in Table 1.

3.4. Hydrographic response to historical precipitation: model setup and calibration

Despite the main objective of this work is the development of a tool to enhance hydrological modeling for design flood, an essential component in evaluating reliability of hydrological models, even simplified, is validation against observed data. Models' performances are usually measured through comparisons with discharge time series at the catchment outlet (Francipane et al., 2012), since the typical lack of information and the limitations of most models to the interior catchment information.

The modeling framework developed here has been calibrated for all the basins previously described, using 44 historical events of precipitation and water level (converted into discharge). These events are not evenly distributed across the three basins considered: 13 events for the two smaller basins, Oreto and Pollina (for a total of 26 events), and 18 events for the largest basin, Platani. Water level data was collected at the basins' outlets from the AdB network, thus demonstrating the capability of the tool to reconstruct also several historical events. We used *Option 3* in the GEO-GLOBAL module to calculate the spatial distribution of flow velocities across the watershed (see Section 2.1.2) and derive the time-area of the basin to convert the runoff into a hydrograph at the basin outlet. Calibration was carried out on two parameters, that are the initial abstraction parameter, I_a, of the CN method and the transfer velocity. For each basin and for each event here considered, the velocities have been amplified (or reduced) by multiplying the velocity layer (see *Option 3*) by ten different values of a calibration coefficient, k_v, ranging between 0.2 and 2. Each of the velocity layers thus obtained has been used to perform simulations by varying I_a and identifying the one that optimally balances metrics relative to peak estimation (relative peak error - RPE) and hydrograph reconstruction (Nash & Sutcliffe Index - NSE; Nash and Sutcliffe, 1970).

Since one of the primary objectives of this work is to develop a framework to generate design flood, the aim of the calibration was to primarily capture the peak of the hydrological response as accurately as possible, which is crucial for flood design purposes. However, following Moriasi et al. (2007), in many cases, the calibration procedure was "very good", with NSE higher than 0.9. Overall, the average NSE values indicate a good performance, ranging between 0.65 and 0.75.

The results showed that the velocities estimated with *Option 3* module are optimal for the Oreto basin, while they need to be multiplied by a small amplification coefficient (i.e., between 1 and 1.25) for the Pollina basin and by a reduction coefficient between 0.5 and 0.65 for the Platani basin. Given the basin sizes, this result could indicate that the developed procedure adapts better to smaller basins than to larger ones. Considering that Sicily often lacks discharge measurements, and, in some cases, the available data are unreliable, these results could provide an indication of the range of amplification (or reduction) coefficients to be used in situations where calibration of the current model is not possible or difficult.

Fig. 8 shows the results for the Oreto, Pollina, and Platani basins when historical data are used. The simulated hydrographs show a good agreement, especially in terms of peak with the observed hydrographs (continuous red curves) with RPE = −4.2 %, and NSE = 0.91 for the Oreto basin, RPE = 0.0 %, and NSE = 0.92 for the Pollina basin, and RPE = −5.3 %, and NSE = 0.98 for the Platani basin.

Table 1
Basins' characteristics.

Characteristics	Oreto	Pollina	Platani
Area [km^2]	71	102	1402
Elevation Range [m]	1184	1765	1540
Mean Elevation [m]	604	928	519
Mean Slope [deg]	18	19.5	11.7
CN_{II}	69.3	68.4	79.6

3.5. Hydrographic response to synthetic precipitation

The tool was used to simulate the response of the Oreto basin at Ponte Parco (see Fig. 7) to a synthetic rainfall with a 100-year return period and a duration equal to the concentration time of the watershed, d_{cr}, as previously calculated in the GEO module, under AMC_{III} soil moisture conditions.

Following the flowchart in Fig. 3, after delineating the basin, the GEO-LOCAL module retrieves information about the homogeneous region and the a_{24} and n parameters of the regionalization procedure by Forestieri et al. (2018) from the DATA module. In this case, the basin lies entirely within the homogeneous region identified as Centre North (see Fig. S3 in the supplementary material) by Forestieri et al. (2018), which is characterized by $h_r(T) = 2.452$ for a 100-year return period. The a_{24} and n layers are then clipped and spatially averaged across the basin, returning values of $a_{24} = 71.3\ mm$ and $n = 0.3625$, which, substituted into equation (6), return a scale factor $\mu(d) = 37.2$ mm. Finally, from equation (5), the rainfall quantile for a 100-year return period and a d_{cr} = 4 h results being equal to $h_{d,T} = 91.3$ mm, increasing to 98.1 mm when considering the climate change factor, F_A, for the period 2023–2050 (Treppiedi et al., 2024a, 2024b). Starting from the adjusted rainfall quantile, the tool constructs the Chicago hyetograph, considering the peak position, r, which is set to 0.25 in this case, and using a time step of 1 h, since $d_{cr} \geq 3$ h.

At this point, assuming AMC_{III} soil moisture conditions, the tool clips and spatially averages CN_{II} in DATA across the basin and calculates the CN_{III} value for the watershed. This value is then used to estimate the runoff using the CN method. In this case, as previously mentioned, we used the tool previously calibrated for the Oreto basin, using *Option 3* in the GEO-GOBAL module to calculate the spatial distribution of flow velocities across the watershed (see Section 2.1.2) and derive the time-area of the basin to convert the runoff into a hydrograph at the outlet section. As a result of the simulation, the tool generates spatially explicit outputs, including basin shapefiles, clipped raster datasets, hyetographs and hydrographs, graphs, and tabular results, as shown in Fig. 9. Finally, Fig. 10 shows the runoff (Fig. 10a) and the discharge at the basin outlet (Fig. 10b) under AMC_{III}.

The tool returned a hydrograph at the Ponte Parco section with a peak value of 409.3 m^3/s, which is close to the value reported by the Sicilian Flood Risk Management Plan (*Piano per la Gestione del Rischio di Alluvioni - PGRA*), equal to 396.5 m^3/s, for the Oreto basin considering a synthetic rainfall event with return period and time of concentration equal to those here used. The peak value here obtained is fully compatible with the PGRA value, especially considering that PGRA refers to the Ponte Corleone outlet, which drains an area of 83 km^2 that is 12 km^2 larger than the 71 km^2 drained at the Ponte Parco outlet, and that we accounted for the effects of climate change through F_A, which plays into an increase in design rainfall. Additionally, we used here AMC_{III} derived from an updated layer of CN_{II} for Sicily, as mentioned in Section 3.2, which provides a lower value of CN_{II} for the Oreto basin compared to the older layer (i.e., 70 vs. 78).

4. Discussion and conclusions

Design floods play a fundamental role in many fields, encompassing the design of hydraulic structures for the management of surface water, such as urban drainage systems, the design of structures aimed at mitigating hydraulic risk, including flood control and retention basins, as well as the development of operational tools for the assessment and management of hydraulic risk. Therefore, given their broad application, design floods are nowadays utilized by both practitioners involved in

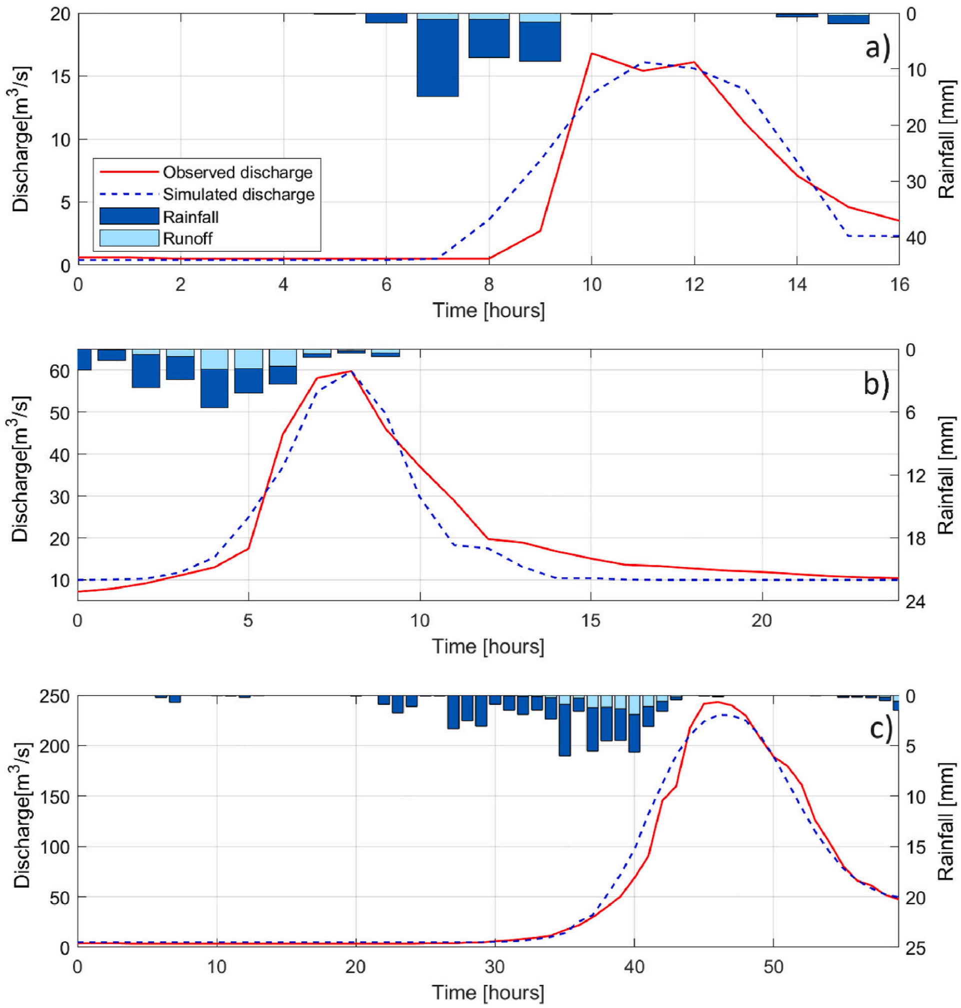

Fig. 8. Calibration for the a) Oreto basin (event recorded between 00:00 and 16:00 on 2015/11/25), b) Pollina basin (event recorded between 03:00 on May 12, 2009, and 03:00 on 2009/12/06), and c) Platani basin (event recorded between 07:00 on 2014/01/31, and 18:00 on 2014/02/02). Dashed blue curves and red continuous curves represent simulated and observed discharges, respectively. (For interpretation of the references to colour in this figure legend, the reader is referred to the Web version of this article.)

hydraulic design and decision-makers engaged in the hydraulic risk assessment, monitoring and management of hydraulic structures.

As emphasized by Pilgrim and Cordery (1992), the estimation of design floods involves a probabilistic assessment of floods for a given return period. Since various combinations of rainfall and basin conditions can result in the same design flood, it is essential to establish a framework that, starting from design rainfall, determines design floods using simple rainfall abstraction and routing models. This framework requires the availability of data for creating the design rainfall to be used as forcing, as well as distributed data to describe the morphological and hydrological characteristics of the basin, and hydrological models, even simplified, for rainfall abstraction and runoff propagation.

In this context, the present study proposes a user-friendly tool that enhances the hydrological flood modeling process by integrating geospatial analysis capabilities, hydrological algorithms, and data, with the primary aim of estimating design floods at any point within a given territory for planning and designing hydraulic and flood management structures or supporting decision-making. The tool, developed and tested for Sicily, comprises four interconnected modules that, upon defining the point for which the design flood is to be determined, enable.

1) the collection, manipulation, and management of input data along with outputs generated by the tool;
2) the definition of the design rainfall (e.g., DDFs and Chicago hyetograph), which also can account for the effects of current and future climate change;
3) the calculation of basin losses, leading to the determination of the net hyetograph;
4) the calculation of the design flood for the selected section.

The integrated workflow, which consolidates multiple processes (e.g., DDF curve derivation, synthetic hyetograph generation, CN method application, distributed UH method) into a single cascade workflow, reduces the need for users to perform these steps separately. The modular and flexible design of the tool allows users to select from various methods of rainfall abstraction and/or runoff routing. In this regard, one of the main advancements of the proposed tool is the possibility to derive a spatially distributed time of concentration layer, which provides a more realistic catchment response to precipitation. More in detail, since this layer strongly relies on the transfer velocities of water along slopes and within the network of a basin, the tool offers the user three options, depending on data availability and quality: from setting a constant flow velocity across the watershed, to defining two different values of velocity for the hillslopes and the network, to finally defining a spatial distribution of flow velocity based on the watershed's morphometric characteristics. To this end, the tool is equipped with updated layers of Curve Number for Sicily and hydrological soil groups,

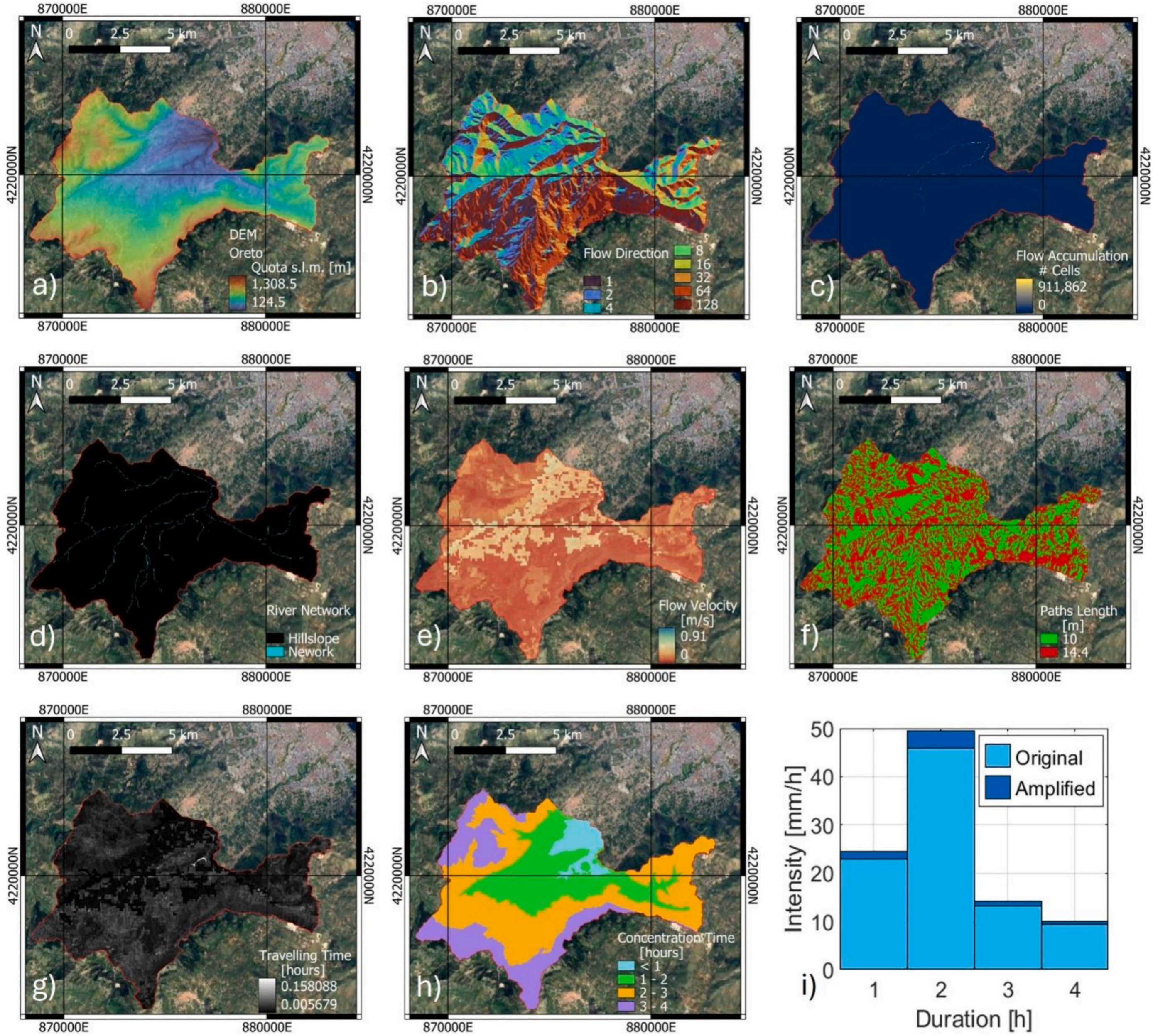

Fig. 9. Spatial outputs obtained by applying the tool to the Oreto basin with outlet at Ponte Parco. a) filled DEM, b) flow directions, c) flow accumulation, d) stream network, e) flow velocity, f) paths length, g) travelling time for each cell, h) concentration time, i) Chicago hyetograph, where the red hyetograph represents precipitation amplified by the climate change factor, F_A, while the blue hyetograph represents original (unamplified by F_A) precipitation. (For interpretation of the references to colour in this figure legend, the reader is referred to the Web version of this article.)

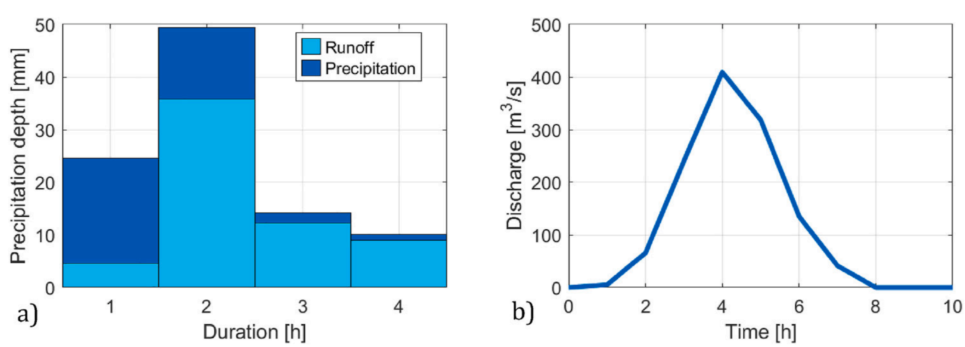

Fig. 10. Response of the Oreto river basin in terms of a) runoff and b) discharge at Ponte Parco when an AMC_{III} soil moisture condition is considered.

derived from the most recent land use/cover and soils layers.

Beyond the primary objective to estimate design floods, the modular structure of the tool allows users to use it for providing additional services that can significantly benefit practitioners, decision-makers, and other professionals. As an example, the tool allows for the use of the RAINFALL module, bypassing all other modules, to determine DDF curves for any point in the study area. This can be very useful, for example, when practitioners need to design hydraulic infrastructures or when hydrological agencies conduct risk assessment and management. If required, the tool allows for the consideration of the effects of climate change projections on the hydrological response of basins by using multiplicative climate correction factors (Martel et al. 2021; Treppiedi et al., 2024a, 2024b), thereby making it possible to anticipate and manage the risk associated with future extreme rainfall events and ensuring the infrastructure can withstand or mitigate the effects of floods expected in the future, especially in urban environments. This is particularly relevant in the context of increasing extreme weather events due to climate change, highlighting the importance of continued model development and application to inform flood mitigation strategies, for example.

Also, the tool allows users to reconstruct historical flood events based on simulations of actual precipitation events. This capability makes it possible to make a rough calibration of the tool for those basins where discharge data are available. Due to the parsimony of the models within the tool, calibration here is intended to verify the physical consistency of the flood hydrographs simulated by the tool, rather than its ability to closely reproduce the observed hydrograph at a control section in the basin, as it is generally required from a hydrological model. In this case, the calibration was performed on just two parameters, which are the initial abstraction parameter, I_a, of the CN method, and the transfer velocity of runoff in the basin, and was carried out for different rainfall events for three different Sicilian basins, returning satisfactory results, particularly for smaller basins. With this respect, by introducing calibration coefficients for the velocity layer in different basins, the study provided some insights for approximating basin responses where discharge data are limited, absent, or unreliable. This makes it possible to calibrate specific modules of the GETAFLOOD tool, extending the model's applicability even to less monitored basins. Even when applied to a synthetic case, the tool returned a peak of the design flood closely matching the results reported by the Sicilian *PGRA*, thus demonstrating its consistency.

At this moment, the tool does not consider artificial reservoirs created by dams. Future versions will allow the user to assess the impact of dams and upstream reservoirs, which may help protect the territory in a time of rapid climate and land-use changes. As an example, this enhancement could allow for evaluating how initial reservoir levels can reduce flooding for specific return periods, making dams more effective for flood control.

Despite being developed and tested for Sicily, the open-source nature of the tool, along with its modular and flexible design, makes it adaptable to be readily applied to other regions worldwide. Of course, some functionalities, such as the spatially distributed flow velocity layer, depend on the availability and quality of morphometric and hydrological data, which may not always be accessible. Additionally, to generate the forcing hyetograph required for deriving hydrographs in synthetic cases or to compute the DDF curves for user-specified return periods, the tool requires input layers derived from a regionalized procedure in line with that proposed by Forestieri et al. (2018) for Sicily.

Furthermore, the application of the tool to reconstruct historical events showed that the procedure developed to estimate distributed velocities adapts better to smaller basins than to larger ones. This provides useful insights into the range of amplification (or reduction) coefficients to be used in situations where calibration of the framework is not possible or is difficult. Further applications in gauged basins in other regions could provide valuable insights into the behavior of the tool at different spatial scales and help refine the range of correction factors needed for the distributed velocities.

Finally, although this work does not introduce a new or inherently innovative model, it provides a valuable framework that integrates data, existing hydrological methods, and GIS functionalities to enhance flood modeling, address common assumptions (e.g., time of concentration and time-area curves), and consider climate change impacts, thus filling a gap in the current literature. One of the greatest advantages of the developed tool is that all these processes, which are typically performed separately by the user during the design flood analysis, are integrated into a single cascade workflow, offering a valuable support in decision-making for hydrological agencies and practitioners.

CRediT authorship contribution statement

Antonio Francipane: Writing – review & editing, Writing – original draft, Software, Conceptualization. **Giuseppe Cipolla:** Software, Data curation. **Dario Treppiedi:** Writing – review & editing, Visualization, Investigation. **Leonardo Valerio Noto:** Writing – review & editing, Supervision, Software, Conceptualization.

Software availability

- Name of software: GETAFLOOD
- **Developers**: Antonio Francipane, Giuseppe Cipolla, Dario Treppiedi and Leonardo V. Noto
- **Contact**: antonio.francipane@unipa.it
- **Date first available**: 2024
- **Software required**: QGIS
- **Program language**: Python 3.9
- **Source code**: Due to copyright restrictions, the code is not available. However, we provide as much detail as possible on the code within the manuscript.

Declaration of generative AI and AI-assisted technologies in the writing process

During the preparation of this work the authors used ChatGPT in order to improve readability and language of the work. After using this tool, the authors reviewed and edited the content as needed and take full responsibility for the content of the publication.

Funding

This study was carried out within the RETURN Extended Partnership and received funding from the European Union Next-GenerationEU (National Recovery and Resilience Plan – NRRP, Mission 4, Component 2, Investment 1.3 – D.D. 1243 August 2, 2022, PE0000005).

Declaration of competing interest

The authors declare that there are no conflicts of interest related to the publication of this paper. The authors have no financial, personal, or professional affiliations that could be perceived to influence the content or conclusions presented in this manuscript.

Acknowledgements

The author acknowledges the support of the Basin Authority of the Hydrographic District of Sicily within the project entitled "*Attività di studio e ricerca per la valutazione dell'impatto dei cambiamenti climatici e l'aggiornamento dell'idrologia di piena in attuazione della direttiva 2007/60*" (Activities of study and research for the evaluation of the climatic change impacts and the update of the flood hydrology in the implementation of guideline 2007/60) — CUP G69J17000830001.

Appendix A. Supplementary data

Supplementary data to this article can be found online at https://doi.org/10.1016/j.envsoft.2025.106497.

Data availability

Due to copyright restrictions, the code and some data are not available. Detailed descriptions of the code and data is provided in the manuscript. Additional information can be provided upon request.

References

Agonafir, C., Lakhankar, T., Khanbilvardi, R., Krakauer, N., Radell, D., Devineni, N., 2023. A review of recent advances in urban flood research. Water Security 19, 100141. https://doi.org/10.1016/j.wasec.2023.100141.

Almeida, I., Kaufmann Almeida, A., Anache, J., Steffen, J., Alves Sobrinho, T., 2015. Estimation on time of concentration of overland flow in watersheds: a review. Geociencias 33, 661–671.

Andrade, C.W.L., Montenegro, S.M.G.L., Montenegro, A.A.A., Lima, J.R.D.S., Srinivasan, R., Jones, C.A., 2021. Climate change impact assessment on water resources under RCP scenarios: a case study in Mundaú River Basin, Northeastern Brazil. Intl Journal of Climatology 41. https://doi.org/10.1002/joc.6751.

Brêda, J.P.L.F., De Paiva, R.C.D., Collischon, W., Bravo, J.M., Siqueira, V.A., Steinke, E. B., 2020. Climate change impacts on South American water balance from a continental-scale hydrological model driven by CMIP5 projections. Clim. Change 159, 503–522. https://doi.org/10.1007/s10584-020-02667-9.

Buchhorn, M., Smets, B., Bertels, L., De Roo, B., Lesiv, M., Tsendbazar, N., Herold, E., Fritz, M., 2020. Copernicus Global Land Service: Land Cover 100m: Collection 3: Epoch 2019: Globe 2020. https://doi.org/10.5281/zenodo.3939050.

Cho, Y., Engel, B.A., Venkatesh, M.M., 2018. A spatially distributed Clark's unit hydrograph based hybrid hydrologic model (Distributed-Clark). Hydrol. Sci. J. 63 (10), 1519–1539. https://doi.org/10.1080/02626667.2018.1516042.

Clark, M.J., 1998. Putting water in its place: a perspective on GIS in hydrology and water management. Hydrol. Process. 12, 823–834. https://doi.org/10.1002/(SICI)1099-1085(199805)12:6<823::AID-HYP656>3.0.CO;2-Z.

Costantini, E.A.C., 2007. Linee guida dei metodi di rilevamento e informatizzazione dei dati pedologici. CRA_ABP, Firenze, Italia, p. 296.

Dang, A.T.N., Kumar, L., 2017. Application of remote sensing and GIS-based hydrological modelling for flood risk analysis: a case study of District 8, Ho Chi Minh city, Vietnam. Geomat. Nat. Hazards Risk 8, 1792–1811, 2017.

Domniţa, M., Crăciun, I., Haidu, I., Magyari-Sáska, Z., 2010. GIS used for determination of the maximum discharge in very small basins (under 2 km2). WSEAS Trans. Environ. Dev. 6, 468–477, 2010.

Evangelista, G., Woods, R., Claps, P., 2023. Dimensional analysis of literature formulas to estimate the characteristic flood response time in ungauged basins: a velocity-based approach. J. Hydrol. 627 (Part B), 130409. https://doi.org/10.1016/j.jhydrol.2023.130409. ISSN 0022-1694.

Fang, X., Thompson, D.B., Cleveland, T.G., Pradhan, P., Malla, R., 2008. Time of concentration estimated using watershed parameters determined by automated and manual methods. J. Irrig. Drain. Eng. 134 (2), 202–211.

Florinsky, I., 2016. Digital Terrain Analysis in Soil Science and Geology. Academic Press.

Forestieri, A., Lo Conti, F., Blenkinsop, S., Cannarozzo, M., Fowler, H.J., Noto, L.V., 2018. Regional frequency analysis of extreme rainfall in Sicily (Italy). Int. J. Climatol. 38, e698–e716. https://doi.org/10.1002/joc.5400.

Francipane, A., Ivanov, V.Y., Noto, L.V., Istanbulluoglu, E., Arnone, E., Bras, R.L., 2012. tRIBS-Erosion: a parsimonious physically-based model for studying catchment hydro-geomorphic response. Catena 92, 216–231. https://doi.org/10.1016/j.catena.2011.10.005.

Giandotti, M., 1933. Previsione delle piene e delle magre dei corsi d'acqua.

González-Álvarez, Á., Molina-Pérez, J., Meza-Zúñiga, B., Viloria-Marimón, O.M., Tesfagiorgis, K., Mouthón-Bello, J.A., 2020. Assessing the Performance of Different Time of Concentration Equations in Urban Ungauged Watersheds: Case Study of Cartagena de Indias, Colombia. Hydrology 7. https://doi.org/10.3390/hydrology7030047.

Grimaldi, S., Petroselli, A., Nardi, F., Alonso, G., 2010. Flow time estimation with variable hillslope velocity in ungauged basins. Adv. Water Resour. 33 (10), 1216–1223.

Grimaldi, S., Petroselli, A., Tauro, F., Porfiri, M., 2012a. Time of concentration: a paradox in modern hydrology. Hydrol. Sci. J. 57, 217–228. https://doi.org/10.1080/02626667.2011.644244.

Grimaldi, S., Petroselli, A., Nardi, F., 2012b. A parsimonious geomorphological unit hydrograph for rainfall-runoff modelling in small ungauged basins. Hydrol. Sci. J. 57 (1), 73–83. https://doi.org/10.1080/02626667.2011.636045.

Gu, L., Yin, J., Slater, L.J., Chen, J., Do, H.X., Wang, H., Chen, L., Jiang, Z., Zhao, T., 2023. Intensification of global hydrological droughts under anthropogenic climate warming. Water Resour. Res. 59, e2022WR032997. https://doi.org/10.1029/2022WR032997.

Horton, R.E., 1933. The role of infiltration in the hydrologic cycle. Trans. AGU 446–460, 14th Ann. Mtg.

Horton, R.E., 1938. The interpretation and application of runoff plane plot experiments with reference to soil erosion problems. Soil Sci. Soc. Am. Proc. J. 1, 401–437.

Ich, I., Sok, T., Kaing, V., Try, S., Chan, R., Oeurng, C., 2022. Climate change impact on water balance and hydrological extremes in the Lower Mekong Basin: a case study of Prek Thnot River Basin, Cambodia. J. Water Clim. Change 13, 2911–2939. https://doi.org/10.2166/wcc.2022.051.

Keifer, D.J., Chu, H.H., 1957. Synthetic storm pattern for drainage design. ASCE Journal of the Hydraulics Division 83 (HY4), 1332.1–1332.25, 1957.

Kirpich, Z., 1940. Time of concentration of small agricultural watersheds. Civ. Eng. 10, 362.

Li, Z.J., Zhang, K., 2008. Comparison of three GIS-based hydrological models. J. Hydrol. Eng. 13 (5), 364–370.

Lindsay, J.B., 2016. Whitebox GAT: A case study in geomorphometric analysis. Comput. Geosci. 95, 75–84. https://doi.org/10.1016/j.cageo.2016.07.003.

Liu, Y.B., Gebremeskel, S., De Smedt, F., Hoffmann, L., Pfister, L., 2003. A diffusive transport approach for flow routing in GIS-based flood modeling. J. Hydrol. 283, 91–106. https://doi.org/10.1016/S0022-1694(03)00242-7.

L'Abate, G., Barbetti, R., Costantini, E.A.C., 2007. 2007 – database for soil observations and pedological units storing, correlating and geoexploring. In: Costantini, E.A.C. (Ed.), Linee guida dei metodi di rilevamento e informatizzazione dei dati pedologici. CNCP 3.0, December 2007. CD-Rom attached to volume. S.EL.CA. Srl, Firenze.

Maidment, D.R., 1993. Developing a spatially distributed unit hydrograph by using GIS. In: Kovar, K., Nachtnebel, H.P. (Eds.), Application of Geographic Information Systems in Hydrology and Water Resources Management, vol. 211. IAHS Publication, Vienna, pp. 181–192.

Maidment, D.R., et al., 1996. Unit hydrograph derived from a spatially distributed velocity field. Hydrol. Process. 10, 831–844. https://doi.org/10.1002/(SICI)1099-1085(199606)-10:6<831::AID-HYP374>3.0.CO;2-N.

Martel, J.-L., Brissette, F.P., Lucas-Picher, P., Troin, M., Arsenault, R., 2021. Climate change and rainfall intensity–Duration–Frequency curves: overview of science and guidelines for adaptation. J. Hydrol. Eng. 26 (10), 03121001. https://doi.org/10.1061/(ASCE)HE.1943-5584.0002122.

Meresa, H., Zhang, Y., Tian, J., Ma, N., Zhang, X., Heidari, H., Naeem, S., 2023. An integrated modeling framework in projections of hydrological extremes. Surv. Geophys. 44, 277–322. https://doi.org/10.1007/s10712-022-09737-w.

Michailidi, E.M., Antoniadi, S., Koukouvinos, A., Bacchi, B., Efstratiadis, A., 2018. Timing the time of concentration: shedding light on a paradox. Hydrol. Sci. J. 63, 721–740. https://doi.org/10.1080/02626667.2018.1450985.

Mishra, Surendra Kumar, Singh, Vijay P., 2013. Soil Conservation Service Curve Number (SCS-CN) Methodology, vol. 42. Springer Science & Business Media, 2013.

Moghadam, S.H., Ashofteh, P.-S., Loáiciga, H.A., 2023. Investigating the performance of data mining, lumped, and distributed models in runoff projected under climate change. J. Hydrol. 617, 128992. https://doi.org/10.1016/j.jhydrol.2022.128992.

Moriasi, D.N., Arnold, J.G., Van Liew, M.W., Bingner, R.L., Harmel, R.D., Veith, T.L., 2007. Model evaluation guidelines for systematic quantification of accuracy in watershed simulations. Transactions of the ASABE 50, 885–900, 2007.

Nash, J.E., Sutcliffe, J.V., 1970. River flow forecasting through conceptual model. Part 1—a discussion of principles. J. Hydrol. 10, 282–290. https://doi.org/10.1016/0022-1694(70)90255-6.

Nonki, R.M., Amoussou, E., Lenouo, A., Tshimanga, R.M., Houndenou, C., 2023. Sensitivity and identifiability analysis of a conceptual-lumped model in the headwaters of the Benue River Basin, Cameroon: implications for uncertainty quantification and parameter optimization. Nord. Hydrol 54, 1036–1054. https://doi.org/10.2166/nh.2023.243.

Noto, L.V., La Loggia, G., 2007. Derivation of a distributed unit hydrograph integrating GIS and remote sensing. J. Hydrol. Eng. 12, 639–650. https://doi.org/10.1061/(ASCE)1084-0699(2007)12:6(639).

O'Callaghan, J.F., Mark, D.M., 1984. The extraction of drainage network from digital elevation data. Comput. Vis. Graph Image Process 28, 323–344.

Perez, G., Gomez-Almeida, I., Kaufmann Almeida, A., Anache, J., Steffen, J., Alves Sobrinho, T., 2015. Estimation on time of concentration of overland flow in watersheds: a review. Geociencias 33, 661–671.

Pilgrim, D.H., Cordery, I., 1992. Flood runoff. In: Maidment, D.R. (Ed.), Handbook of Hydrology. McGraw-Hill, New York, pp. 9.1–9.42.

Righini, G., Costantini, E.A., Sulli, L., 2001. La banca dati delle regioni pedologiche italiane. Boll. Soc. It. Scienza del Suolo 50 (Suppl. l.), 261–271.

Rodríguez-Iturbe, I., Rinaldo, A., 1997. Fractal River Basins: Chance and Self-Organization. Cambridge University Press, New York.

Sahu, M.K., Shwetha, H.R., Dwarakish, G.S., 2023. State-of-the-art hydrological models and application of the HEC-HMS model: a review. Model. Earth Syst. Environ. 9, 3029–3051. https://doi.org/10.1007/s40808-023-01704-7.

Salimi, E.T., Nohegar, A., Malekian, A., Hoseini, M., Holisaz, A., 2017. Estimating time of concentration in large watersheds. Paddy Water Environ. 15, 123–132. https://doi.org/10.1007/s10333-016-0534-2.

Shepard, D., 1968. A two-dimensional interpolation function for irregularly-spaced data. In: Proceedings of the 1968 ACM National Conference, pp. 517–524, 1968.

Sherman, LeRoy K., 1932. Streamflow from rainfall by the unit-graph method. Eng. News Record 108, 501–505.

Soil Conservation Service (SCS), 1957. 1972. National Engineering Handbook, Section 4: Hydrology. Washington, D.C.: SCS.

Tarquini, S., Isola, I., Favalli, M., Mazzarini, F., Bisson, M., Pareschi, M.T., Boschi, E., 2007. TINITALY/01: a new triangular irregular network of Italy. Ann. Geophys. 50 (3), 407–425.

Thakur, J.K., Singh, S.K., Ekanthalu, V.S., 2017. Integrating remote sensing, geographic information systems and global positioning system techniques with hydrological modeling. Appl. Water Sci. 7, 1595–1608. https://doi.org/10.1007/s13201-016-0384-5.

Treppiedi, D., Francipane, A., Noto, L.V., 2024a. Valutazione delle curve di probabilità pluviometrica per il XXI secolo in Sicilia. Atti del XXXIX Convegno Nazionale di Idraulica e Costruzioni Idrauliche IDRA2024 Parma 15–18 settembre 2024. ISBN: 979-12-210-6941-9. DOI: 10.5281/zenodo.13584918 (in Italian).

Treppiedi, D., Francipane, A., Noto, L.V., 2024b. Projecting depth-duration-frequency curves for future climate: a case study in the mediterranean area. Water Resour. Manag. https://doi.org/10.1007/s11269-025-04162-1, 2025.

U.S. Department of Agriculture, 2009. Natural resources conservation service. Hydrology, National Engineering Handbook, Part 630. http://directives.sc.egov.usda.gov/viewerFS.aspx?hid=21422.

U.S. Department of Agriculture Soil Conservation Service, 1986. Urban Hydrology for Small Watersheds. Tech. Release No., 55, Washington, DC, June, 1986.

Van Rossum, G., Drake, F.L., 2009. Python 3 reference manual. CreateSpace, Scotts Valley, CA.

Velásquez, N., Vélez, J.I., Álvarez-Villa, O.D., Salamanca, S.P., 2023. Comprehensive analysis of hydrological processes in a programmable environment: the watershed modeling framework. Hydrology 10, 76. https://doi.org/10.3390/hydrology10040076.

Wang, L., Liu, H., 2006. An efficient method for identifying and filling surface depressions in digital elevation models for hydrologic analysis and modelling. Int. J. Geogr. Inf. Sci. 20 (2), 193–213.

Wang, L., Wang, Z., Liu, C., Bai, P., Liu, X., 2018. A flexible framework HydroInformatic modeling system—HIMS. Water 10, 962. https://doi.org/10.3390/w10070962.